

## Langmuir probe measurements of electron density and electron temperature in early stage of a laser-produced carbon plasma

C. Hong\*, H. B. Chae, S. B. Lee, Y. J. Han, J. H. Jung, B. K. Cho, and H. Park  
*Division of Mathematics and Physics, Soonchunhyang University, Asan 336-745, Korea*

C. K. Kim  
*Department of Electrical and Electronic Engineering, Soonchunhyang University, Asan, 336-745 Korea*

S. O. Kim  
*Department of Physics, Seonam University, Namwon 590-711, Korea*

E-mail : schpch@asan.sch.ac.kr

(Received 17 February 2000, Accepted 24 March 2000)

Langmuir probe measurements of electron density, electron temperature, and plasma potential are made in the early stages ( $< 5 \mu\text{s}$ ) of a laser ablated plasma plume, in which a positive current from positive ions and a electron current are overlapped. The plasma was produced by focusing the second harmonic, 532nm, of Q-switched Nd:YAG laser on a high purity carbon target. Then the laser intensity on the target was of  $\sim 1.6 \times 10^{15} \text{ W/cm}^2$ . The measured electron densities and temperatures are  $\sim 2 \times 10^{11} \text{ cm}^{-3}$  and  $\sim 3 \text{ eV}$ . In particular, the phenomenon that the electron temperature decreased and then increased was observed. It could be well explained that this phenomenon occurred in the process of inverse Bremsstrahlung of free electrons in plasma. Additionally, the plasma potential ( $> 11 \text{ V}$ ) was higher than the published values.

*Keywords* : Langmuir probe, laser ablation, carbon film, plasma

### 1. INTRODUCTION

The last two decades have been considerable interest in pulsed laser deposition (PLD) film because of simple experimental setup for deposition and possibility to prepare a wide variety, 280, of materials in thin film form[1]. Even though the deposition conditions such as laser intensity on a target, laser wavelength, and pressure in vacuum chamber are equivalent but only used vacuum system is different, it has been reported that physical properties of deposited thin films can be quite different and, moreover, deposition conditions to improve the film quality become different in a few cases[2]. For example, there has been discrepancy on the substrate temperature to deposit diamond-like carbon films with high  $sp^3/sp^2$  ratio. Still not known why such controversy exists, it can be guessed that some factors have made great influences on the deposition processes of films. Therefore, it can be concluded that to use plasma parameters for specifying optimum conditions is more general than to control deposition conditions. To do so, it is necessary to diagnose the laser produced plasma with ion

probes and/or optical probes.

One of typical ion probes, Langmuir probe, gives informations, including the electron density, electron temperature, Debye length, and plasma potential, on electrons in the plasma. As the first step to determine the charge state of ions and ion density in the plasma, informations on electrons are absolutely necessary because positive ions and electrons are overlapped in early stage of plasma.

In the laser-produced plasma the electron current exists for quite longer time than ion current so that the plasma parameters can be calculated in late stage of plasma in some published papers[3]. In this paper, a reason that those parameters can be obtained in early stage will be discussed in Sect. 4. For such a short time interval, of course, it is of importance to interact the plasma with an intense laser beam. Here only qualitative analysis can be possible and, in the future, it will be expected that quantitative analysis can be possible by applying the transport theory to the laser plasma.

## 2. THE EXPERIMENTAL

A schematic experimental arrangement to deposit diamond-like carbon (DLC) films by the pulsed laser deposition (PLD) technique is shown in Fig. 1. The laser beam of frequency-doubled Nd:YAG laser (532nm) was focused on high purity (99.997%) graphite target in spot size of  $\sim 10 \mu\text{m}$  with a plane-convex lens (focal length of 28cm) and the target was ablated to produce carbon plasma in the form of carbon clusters. Then the laser intensity on the target was calculated to be  $1.6 \times 10^{15} \text{ W/cm}^2$ . It is well accepted that, as the laser intensity becomes more intense, the plasma consists of much better ionized atoms and the kinetic energies of those atoms become higher. The laser intensity of this order or above has been used mainly to generate fast electrons [4,5], which can play a very important role for the purposes of laser thermonuclear fusion and for an injector of high-current pulsed accelerators as cathode. Then, the energy of the electrons that absorbed such intense laser radiation was observed to be more than  $10^2 \text{ keV}$ . With the detection system used here such fast electrons could not be measured and only the time behavior of slow electrons was investigated.

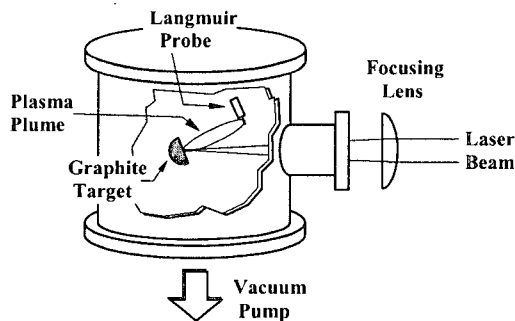


Fig. 1. Schematic diagram for a Langmuir probe setup. The graphite target is connected to the linear feedthrough, which is controlled by a stepper motor outside the vacuum chamber. The probe is placed in the normal direction with respect to the graphite.

The target used here was so connected to the chamber and grounded that electrically free field inside the chamber where the plasma moved was formed. A Langmuir probe was positioned 5cm in the normal direction from the laser spot on the target. The repetition rate of the laser was 10Hz and a laser pulse carried the energy of 500 mJ. The laser beam was irradiated on the target with the incidence angle of  $25^\circ$ . Cutting a graphite cylinder of 1 cm diameter into two pieces along its axis, one was used as target. It was mounted on a linear translator moving at rate of 1.5" for 22 minutes to prevent the target to be punctuated. The

Langmuir probe was a cylindrical tungsten wire, which was  $42.7 \mu\text{m}$  ( $\sim 2 \text{ mil}$ ) in diameter and was 5 mm in length. The probe tip was supported by a ceramic tube, which was 2.5 mm in diameter and was tightly enclosed by a glass tube.

Whenever the laser was shot in pulse shape (pulse width 6 ns), a synchronized output pulse from the laser console was used to trigger external detecting devices. But time jitter between the laser pulse and the trigger pulse may inhibit the precise timing measurement. Fortunately, when the laser beam reflected from the target or the ultra-violet (UV) light emitted from promptly produced plasma illuminates the Langmuir probe, the photoelectrons can be ejected from the surface of the metal probe to remain its surface as the positive charge state that is measured in positive voltage signal through oscilloscope. So the time that the photoelectron signal began to appear was considered to be zero time in which the laser was shot. It has been reported that such method to calibrate the zero time was mentioned in many published papers [6~8].

Because high voltage pulse for the pulse operation of laser could induce the electromagnetic interferences on some detecting devices, those might be a stumbling block to measure the signal of ion probe. Thus, by using the coaxial cable for high frequency telecommunication, this problem has been completely overcome. All cables used in Fig. 2 are those ones.

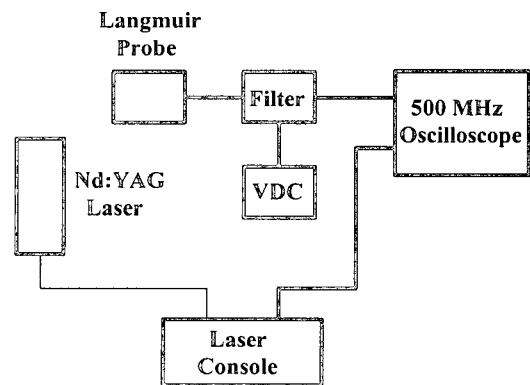


Fig. 2. Block diagram to trigger the oscilloscope via the Q-switch synchronous output of the laser console. The thick lines are the sufficiently shielded cables, suitable for high frequency telecommunications, to overcome noise problem.

Each signal of Langmuir probe was measured with the load resistor,  $50 \Omega$ , of 500 MHz oscilloscope (HP 54520A) varying the bias potential to the probe from -10 V to 10 V in 1 V step. In addition to that the time spectra were also taken at +17 V and -17 V bias potential. The plasma was not repeated in the same shape and stable in each laser shot, so the signals were averaged over 128 laser pulses. However, totally 23 time spectra were used to calculate the time-evolved plasma parameters

### 3. THEORY

The Langmuir probe which was developed to provide electron temperature and density informations in nonflowing plasmas is one of the oldest plasma diagnostics. In particular, it has the advantages of both not disturbing plasma and providing local information in plasma[9]. In order to operate the probe under the non-disturbing condition the probe size should be as small as possible but sufficiently large to see collected current. According to the paper of reference 2, the Langmuir probe theories that apply to static and non-flowing plasma can be used in flowing plasma provided the ratio of the electron thermal velocity,  $v_{th}$ , reaching the probe, and the local flow velocity,  $v_1$ , is at least over 3. Considering the experimental values of the electron temperature and arrival time at the probe ( $T_e \sim 4$  eV and  $v_1 \sim 5 \times 10^4$  m/s) yield that the ratio is  $R \sim v_{th} / v_1 = \sqrt{3kT_e / m_e} / v_1 \sim 30$  and Langmuir probe theories that govern static and non-flowing plasma can be used to analyze the experimental results of present study.

The collision of electrons with particles such as ions, neutrals and other clusters in the laser plasma is of importance in that the values of the electron density and its scattering cross section determine which theories can be applied for analysis of the plasma. The mean free path,  $\lambda_c$ , of free electrons in the plasma can be written by

$$\lambda_c \approx \frac{1}{n_g \sigma} \quad (1)$$

where  $n_g$  is the gas density and  $\sigma$  corresponds to the cross section of atom-electron collision.  $n_g$  is of the same order as the electron density if the plasma consists of only ions and electrons and, also, ions are singly ionized. Using  $\sigma \sim 10^{-18}$  m<sup>2</sup> from the references [1, 3, 10, 11] and  $n_g \sim 10^{18}$  m<sup>-3</sup> seen later, the mean free path is roughly  $\lambda_c \sim 1$ m. That is quite large compared to Debye length,  $\lambda_D$ , known as  $\sim 2$   $\mu$ m later. Thus the collisionless, thin sheath theory can be used to analyze the data in our experiment. In addition, the radius, 21.8  $\mu$ m, of the probe was so larger than the Debye length and smaller than the mean free path that large probe analysis is appropriate[11]. Thus complicated theories that involves calculations of particle trajectories through the sheath need not to be considered. Summarizing theories for the plasma analysis discussed so far, it can be

concluded that (1) nearly all particles reaching the sheath boundary are collected by the probe[12] and (2) the trajectories of particles reaching the probe are not complicated.

At a given time the current drawn by the probe can be written as

$$I = I_e + I_{ion} \quad (2)$$

with  $I = I_{0e} \exp(e(V - V_p) / kT_e)$  and  $I_{ion} = \sum I_{0ion,n} \exp(-q_n (V - V_{pion,n}) / kT_{ion})$  in the retarding regime where the probe potential,  $V$ , is less than the electron plasma potential  $V_p$  and larger than the ion plasma potential  $V_{pion,n}$ . In Eq. 2  $I_{0e}$  and  $I_{0ion}$  are the saturation currents of electrons and ions, respectively, and  $q_n$  represents the charge state of ionized carbon atoms. Of course, the fact that the currents satisfy these relations is based on the fact that both electrons and ions show the Maxwellian distributions. In Eq. 2 there will be several ionization states, however, associated ion plasma potentials might be different. As the probe potential increases gradually and, finally, reaches the electron plasma potential,  $V_p$ , the probe current may be called electron saturation current and then the electron current can be described by

$$I_{0e} = \frac{1}{4} n_e e \bar{v} A, \quad (3)$$

where  $A$  is the effective probe area to collect the electrons,  $n_e$  is the electron density, and  $\bar{v}$  is the electron velocity given by

$$\bar{v} = \sqrt{\frac{8kT_e}{\pi m_e}}, \quad (4)$$

where  $m_e$  and  $T_e$  are the electron mass and temperature, respectively. For simplicity and data treatment, we assume that ions are almost singly ionized carbon atoms. When the probe potential is larger than the electron plasma potential, the probe current will increase linearly according to that potential. Thus this behavior is called acceleration regime for electrons. In the case of ions the same relations hold with change of variables as  $T_e \rightarrow T_{ion}$ ,  $V_p \rightarrow V_{pion,n}$ ,  $e \rightarrow -q_n$ , and  $I_0 \rightarrow I_{0ion}$  in Eq. 2.

On the other hand taking the logarithm on Eq. 2 and

differentiating it with respect to the probe potential,  $V$ , the result becomes

$$\frac{d \ln I}{dV} = \frac{I_e \frac{e}{kT_e} - I_{ion} \frac{e}{kT_{ion}}}{I_e + I_{ion}} \quad (5)$$

in the retarding regime ( $V_{pion,n} < V < V_p$ ). Therefore only in the case to satisfy the condition  $I_e \gg I_{ion}$ , Eq. 5 becomes  $d \ln I / dV \approx e / kT_e$  and thus the electron temperature can be calculated. When the electron signal and the ion signal are overlapped, the electron temperature cannot be determined in principle unless the plasma parameters on ions are known. But it is really impossible to specify those parameters because of large statistical errors. Even though the ion plasma potentials cannot be found precisely from experimental data, it can be mentioned that those exist below 0 V. Thus, the second term on the right hand side in Eq. 2 decreases rapidly with the probe potential. This fact leads that I-V curves to indicate the electrons and ions are so sufficiently separated that they can be considered to be independent. Due to this reason the electron temperature can be calculated by differentiating the collected current in logarithm scale with the probe potential as mentioned above. However, the criterion to calculate the electron temperature in this way is whether the collected current is still positive at the probe potential above 0 V. In our data this condition is satisfied 260 ns after the laser shot. It can be concluded that the ion current affects so much to determine the electron temperature. Also, the electron number density can be obtained by using Eq. 3 because the electron velocity  $\bar{v}$  has been given by  $T_e$  in Eq. 4.

The electron current in the electron acceleration regime ( $V > V_p$ ) can be written as [10]

$$I_e = n_e e A \left( \frac{kT_e}{2\pi m_e} \right)^{1/2} \frac{2}{\sqrt{\pi}} \left( 1 + \frac{e(V - V_p)}{kT_e} \right)^{1/2} \quad (6)$$

Eq. 6 means that the square of the electron current in the electron acceleration regime is proportional to the probe potential, where the slope gives the way to determine the electron density,  $n_e$ . In two regimes, acceleration regime and retarding regime, the electron currents will be equivalent at the electron plasma potential.

The Debye length is defined as  $\lambda_D = \sqrt{kT_e / 4\pi e^2 n_e}$  [9,13] and can be calculated by using the electron temperature and density discussed so far.

#### 4. RESULTS AND DISCUSSION

Ions and electrons can contribute the current and overlap in time scale. In Fig. 3 the signal of positive ions and electrons are shown. The magnitude of electron signal is larger than that of ions and it remains in wide time range. After 5  $\mu$ s, ion signal becomes negligibly small compared to electron signal. However, in early stage ion signal and electron signal are comparable. Thus it is difficult to specify the plasma parameter of electron in early stage of plasma. Because of this fact Hendron *et al.* [2] could find the plasma parameters only from 5  $\mu$ s after the production of plasma. Our main concern in present study is to specify the plasma parameters in early stage shorter than 5  $\mu$ s. To overcome this problem, firstly consider the error to measure the electron temperature. I-V characteristic curves of the probe can be derived from Eq. 2

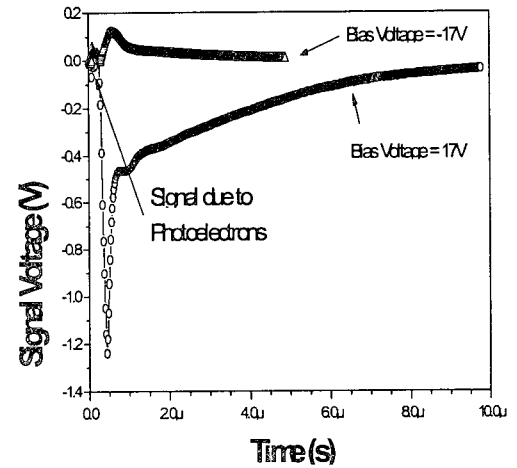


Fig. 3. Signal voltages of the Langmuir probe, with its bias potential at + 17 V and - 17 V, across the load resistor, 50  $\Omega$ , of the oscilloscope

The relation of the electron saturation current,  $I_0$ , to the ion saturation current,  $I_{0ion}$ , is  $(I_{0ion} / I_{0e})_{langmuir} = \sqrt{m_e T_{ion} / m_i T_e}$  [14] and, inserting this equation to Eq. 5 and assuming that  $I_{ion} / I_{0e} \approx I_{0ion} / I_{0e}$ , the resulting equation can be written as

$$\frac{d \ln I}{dV} \approx \frac{e}{kT_e} - \frac{m_e}{m_i} \frac{I_e}{I_{0ion}}, \quad (7)$$

where  $m_i$  is the ion mass and, in present paper, it is assumed to be the mass of single carbon atom. From Koo and Hershkowitz[14] the ratio of the electron saturation current to the ion saturation current,  $I_{0e}/I_{0ion}$ , collected by the probe is given by  $I_{0e}/I_{0ion} = 28\sqrt{\mu_{eff}} \text{ (amu)} \approx 97$ . Therefore, inserting this value and the ratio of electron mass to ion mass to Eq. 7, the value of the second term on the right hand becomes nearly  $4.4 \times 10^{-3}$  when the ion signal and the electron signal are overlapped. As discussed later, the typical value of the slope of  $d \ln I / dV$  at  $1 \mu s$  is  $\sim 0.245$ . This value is much greater than the value from contribution due to the ion,  $4.4 \times 10^{-3}$ . Thus even though the signals due to the ion and electron are overlapped, it can be considered that such a contribution does not make a big disturbance to determine the electron temperature. Fig. 4 shows the temporal evolving of the electron temperature. The electron temperature has the two small peaks at  $420 \text{ ns}$  and  $720 \text{ ns}$  and has a minimum at  $2.2 \mu s$ . After that it increases up to  $7.22 \mu s$  and then decreases slowly. In general, the electron temperature is related with the standard deviation of velocity distribution, which is proportional to  $\sqrt{T_e}$ . Thus, lower is the electron temperature, narrower is the standard deviation of velocity distribution. From the time for electrons to arrive at the probe, the corresponding energy is estimated to  $\sim 8 \text{ meV}$  kinetic energy. Therefore typical thermal energy,  $\sim 3 \text{ eV}$ , of electrons as shown in Fig. 4 is much larger than their kinetic energy. The kinetic energy relating to the arrival time of electron to target should be equal to the velocity of the center of mass velocity approximately due to the collective motion of all electrons. The electron temperature represented as thermal energy is related to the velocity broadening with respect to the velocity of the center of motion. Thus the velocity distribution of electrons has wide broadening distribution about nearly rest center-of-mass.

The energy of laser beam is partially absorbed by relatively fast moving electrons at the early stage of plasma. As a result, that makes some electrons slow. The phenomena of absorption of laser beam by electrons are called inverse Bremsstrahlung (IB), which can occur in the condition that laser beam are sufficiently intense. In this process many photons are involved so that electrons move finally toward the direction of propagation of laser beam. Accordingly the velocity distribution of electrons is changed and then the velocity broadening becomes wider so that the electron temperature begins to increase. In other word the energy of laser beam absorbed by free electrons contributes to heat the plasma.

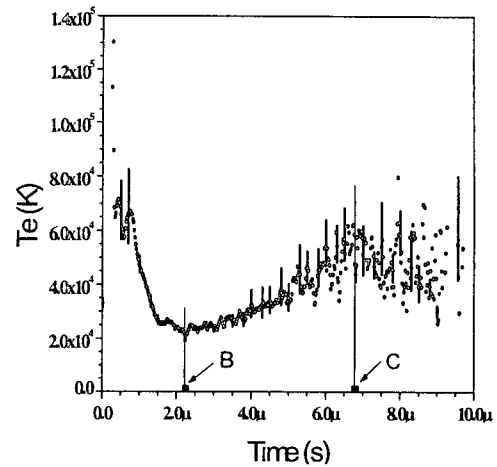


Fig. 4. The time behavior of electron temperature. The time zero indicates when the laser is fired

The electrons experienced like this process can have more chances to make collisions with followed neutral particles or ions and enhance the quality of plasma or ionize the neutral particles. Then the electrons scattered with particles have larger change of velocity so the electron temperature would become high. This phenomenon is indicated in the region between B and C in Fig. 4. Beyond C the electrons are freely expanded and the electron temperature is dropped with time. Thus in the time interval in which electron signal and ion signal are not overlapped this phenomena could not be measured in experiment. In a previous work the electron temperature in early stage was measured but we do not know that our explanation can be adopted because of less data point in that paper. However, up to our knowledge this phenomenon is mentioned here. In Fig. 3 the prompt peak is considered to be the contribution of electrons that do not experience IB. In future work this phenomenon should be treated quantitatively with the transport theory.

As mentioned in other papers we cannot confirm that the electron temperature in later stage varies as  $t^{-3}$  because of lack of data.

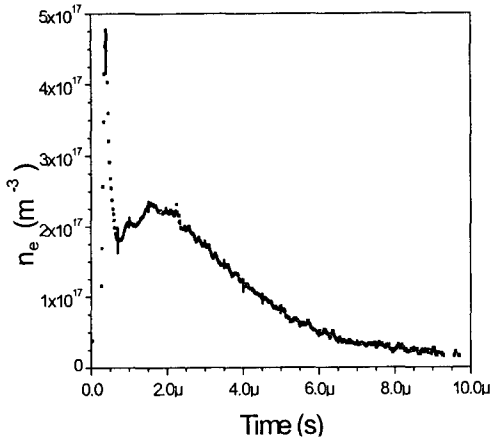


Fig. 5. The number density showing the time evolving behavior of transient plasma.

Fig. 5 represents the electron number density as a function of elapsed time. Here there are two peaks which are clearly distinct. Fitting the data after  $6 \mu\text{s}$  the electron number density shows the time function as  $t^{-n}$ , where  $n=2.08$ . Time dependence like this is coincident with the results of Harilal et al. ( $n = 2$ )[15]. Therefore at later stage of plasma the electrons behaves as expanding adiabatically. Some papers[15] mentioned that even though theoretical model gives the value of  $n=3$ , they used  $n=2$  which show the discrepancy. Based on this time behavior of electron number density the expansion can be considered to be one-dimensional one. To prove this fact let's describe the electron number density in terms of elapsed time. The one-dimensional velocity distribution of electrons with stream velocity of  $v_0$  is described by

$$n_e(v) = A e^{-m_e(v-v_0)^2/2kT_e}, \quad (8)$$

where  $A$  is a constant related to the total number of electrons produced by a laser pulse. What we measure is  $n_e(t)$ . Clearly integration of number density is equal regardless of time domain or velocity domain, that is,

$$\int_{v_1}^{v_2} n_e(v) dv = \int_{t_1}^{t_2} n_e(t) dt \quad (9)$$

In Eq. 9 a velocity corresponds to unique time,  $v_1 \leftrightarrow t_1$  and  $v_2 \leftrightarrow t_2$ . Thus, from Eq. 9 the following equation is derived.

$$n_e(t) = n_e(v) \left| \frac{dv}{dt} \right|, \quad (10)$$

where the absolute value is necessary because the increase of electron velocity corresponds to shorter arrival time to the probe. The velocity can be described in time by using the relation of  $t = L/v$ , where  $L$  is the distance of target-probe. Inserting this relation and Eq. 8 into Eq. 10 results in

$$n_e(t) = B t^{-2} e^{-m(L/t-v_0)^2/2kT_e}, \quad (11)$$

where  $B = AL$ . When the time is sufficiently long the exponential in Eq. 11 is so nearly independent of time that we can consider it as constant. Therefore the electron number density is proportional to  $t^{-2}$  at late stage of plasma expansion. This result is well in agreement with that deduced from the experimental data. In Eq. 10  $n_e(t)$  is obtained from the analysis of experimental data. As we can see, there are two main peaks in Fig. 5. The prompt peak in Fig. 5 is caused by the electrons that do not interact with the intense laser beam because they are produced due to the rising edge of laser pulse. On the other hand the broad peak are the product of electrons in the process of IB. Thus the stream velocities corresponding to each peaks should be different. Since the absorption coefficient of laser beam by free electrons due to IB process is given by[15]

$$\alpha_{ib} (\text{cm}^{-1}) = 1.37 \times 10^{-36} \lambda^3 n_e^3 T_e^{1/2} \quad (12)$$

where  $\lambda$  is the wavelength of used laser in  $\mu\text{m}$ , particularly it is very sensitive to electron number density. Therefore IB process can occur at the time in which the electron number density reaches maximum,  $\sim 1.8 \mu\text{s}$ . Then the amount of energy absorbed by electrons is a few mJ per laser pulse. The interactions of the plasma with the laser beam are to reduce the laser energy to reach the target so that the ablated rate of target material would decrease. Thus after then the electron number density would decrease with time as shown in Fig. 5.

Absorption mechanisms to occur in such processes are given as followings : (1) Inverse-Bremsstrahlung absorption via free electrons, (2) photo-ionization with multi-photon absorption, and (3) recombination of carbon ions and electrons.

As shown in Fig. 4 and Fig. 5 the evolutions of electron temperature and the number density can be explained well only by using IB process.

The velocity distribution of electrons is shown in Fig. 6

which is obtained by coupling Eq. 10 and Eq. 11. In Fig. 6 the most probable velocity is nearly  $10^4$  m/s, whose kinetic energy corresponds to 0.32 meV.

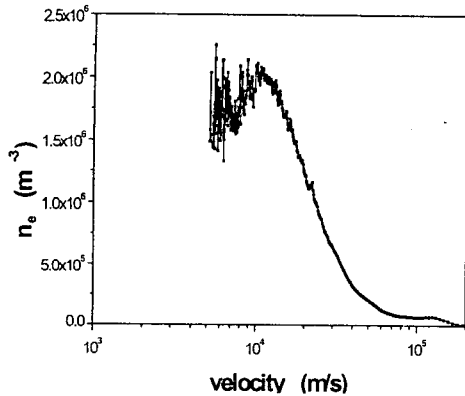


Fig. 6. The electron number density vs its velocity.

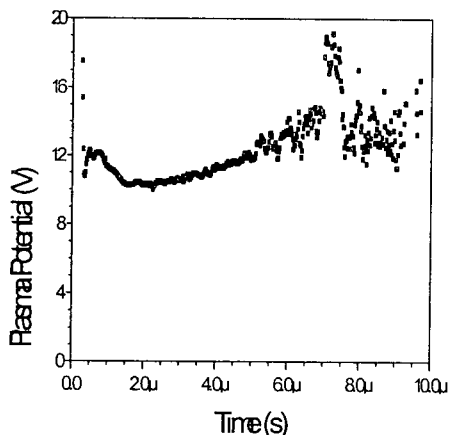


Fig. 7. Time behavior of the plasma potential that is derived from the I-V curves of the Langmuir probe.

The plasma potential with time is shown in Fig. 7. It resembles the time behavior of the electron temperature and, from this fact, it becomes explicit that its time behavior is due to the same mechanism, IB process.

With the definition of Debye length discussed in Section 3 it was derived from the electron temperature and the electron density and shown in Fig. 8.

Since the Debye length means the degree to shield the external electric field near the boundary of the plasma, the electrons and the ions, consisting of the plasma, can be selectively separated into their energies and charge states even by the ion probe equipped with a energy-selective device.

## 5. CONCLUSIONS

In the plasma produced by the irradiation of 532 nm Q-switched Nd:YAG laser beam onto the graphite target, the electron temperature and density are measured with the Langmuir probe and, in particular, the electron temperature shows the time behavior which rapidly decreases upto  $\sim 2 \mu\text{s}$  and then slowly increases until 8  $\mu\text{s}$ . Finally it decreases after that. Even in the early stage of plasma at which the electron current and the ion current are overlapped, it is evident that the electron temperature can be measured precisely. Also, it is shown that the phenomena that the electron temperature increases with time can be explained well by the inverse Bremsstrahlung of intensive laser beam via free electrons in the laser-produced plasma. Typical electron temperature is in the range of 2  $\sim$  7 eV.

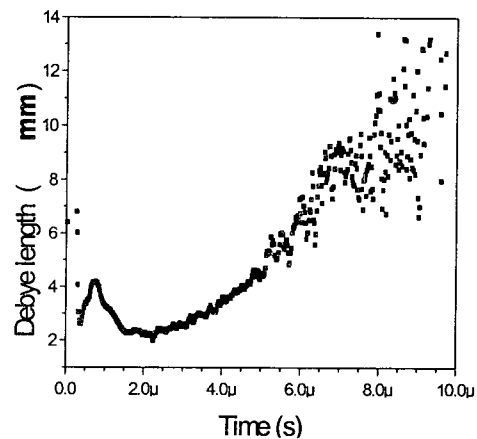


Fig. 8. The time behavior of the Debye length in the laser-produced plasma.

From the electron density the slow and fast electron components are clearly shown. The electron density in the late stage is followed by the power law of  $t^{-2}$ . Then this behavior indicates that the electron can be treated with one-dimensional Maxwellian distribution function.

The plasma potential also is obtained from the I-V characteristic curve of the probe and is ranged to be typically 11  $\sim$  17 V.

The Debye length and the plasma potential show the similar time behavior as the electron temperature.

## ACKNOWLEDGMENTS

This work is supported in part by the Ministry of Information Communication of Korea ("Support Project of University foundation research<'99>" supervised IITA). The authors are thankful to professor D. Ahn, Soonchunhyang University, for his technical assistance.

## REFERENCES

- [1] Physics Abstracts search (1993 ~ now).
- [2] A. A. Voevodin and M. S. Donley, "Preparation of amorphous diamond-like carbon by pulsed laser deposition: a critical review", *Surf. Coat. Technol.*, Vol. 82, p. 199, 1996.
- [3] J. M. Hendron, C. M. O. Mahony, T. Morrow, and W. G. Graham, "Langmuir probe measurements of plasma parameters in the late stages of a laser ablated plume", *J. Appl. Phys.*, Vol. 81, No. 5, p. 2131, 1997.
- [4] V. V. Ivanov, A. K. Knyazev, A. V. Kutsenko, A. A. Matsveko, Yu. A. Mikhalov, V. P. Osetrov, A. I. Popov, G. V. Sklizhov, and A. N. Starodub, "Investigation of the generation of high-energy electrons in a laser plasma", *JETP.*, Vol. 82, No. 4, p. 677, 1996.
- [5] E. Lefebvre and G. Bonnaud, "Nonlinear electron heating in ultrahigh-intensity laser-plasma interaction", *Phys. Rev. E.*, Vol. 55, No. 1, p. 1011, 1997.
- [6] T. N. Hansen, J. Schou, and J. G. Lunney, "Angular distributions of silver ions and neutrals emitted in vacuum by laser ablation", *Europhys. Lett.*, Vol. 40, No. 4, p. 441, 1997.
- [7] J. Diaz, S. Ferrer, and F. Comin, "Role of the plasma in the growth of amorphous carbon films by pulsed laser deposition", *J. Appl. Phys.*, Vol. 84, No. 1, p. 572, 1998.
- [8] R. C. Issac, P. Gopinath, G. K. Varier, V. P. N. Nampoore, and C. P. G. Vallabhan, "Twin peak distribution of electron emission profile and impact ionization of ambient molecules during laser ablation of silver target", *Appl. Phys. Lett.*, Vol. 73, No. 2, p. 163, 1998.
- [9] D. B. Chrisey and G. K. Hubler (eds.), *Pulsed Laser Deposition of Thin Films*, John Wiley, New York, 1994. Chap. 5.
- [10] I. Weaver, G. W. Martin, W. G. Graham, T. Morrow, and C. L. S. Lewis, "The Langmuir probe as a diagnostic of the electron component within low temperature laser ablated plasma plumes", *Rev. Sci. Instrum.* Vol. 70, No. 3, p. 1801, 1999.
- [11] E. A. Brinkman, K. R. Stalder, and J. B. Jeffries, "Electron densities and temperatures in a diamond-depositing direct-current arcjet plasma", *J. Appl. Phys.*, Vol. 81, No. 3, p. 1093, 1997.
- [12] W. Lochte-Holtgreven (eds.), *Plasma Diagnostics*, AIP Press, New York, 1995. Chapt. 2.
- [13] M. A. Lieberman and A. J. Lightenberg, *Principles of Plasma Discharges and Materials Processing*, John Wiley, New York, 1994. Chapt. 2.
- [14] B. W. Koo and N. Hershkowitz, "Langmuir probe in low temperature, magnetized plasmas: Theory and experimental verification", *J. Appl. Phys.*, Vol. 86, No. 3, p. 1213, 1999.
- [15] S. S. Harilal, C. V. Bindhu, Riju C. Issac, V. P. N. Nampoore, and C. P. G. Vallabhan, "Electron density and temperature measurements in a laser produced carbon plasma", *J. Appl. Phys.*, Vol. 82, No. 5, p. 2140, 1997.